Application of 3-D Velocity Measurement of Vessel by VI-GPS for STS Lightering

Y. Yoo & E. Pedersen
Norwegian University of Science and Technology, Trondheim, Norway

K. Tatsumi
Hiroshima National College of Maritime Technology, Hiroshima, Japan

N. Kouguchi
Kobe University, Kobe, Japan

Y. Arai
Marine Technical College, Ashiya, Japan

ABSTRACT: A lightering operation is a type of Ship-To-Ship (STS) operation where two ships are together in open waters and transfer the cargo e.g. crude oil, LNG. High skills and experience are required by the human operators as no relevant equipment for determining the relative speeds and distances with sufficient accuracies has been implemented. The officer in charge of an STS lightering takes the decision on adequate maneuvering orders based on predominantly visual observations during the final approach. Landing on all fenders simultaneously is an objective in order to minimize ship-fender contact forces, but this is rather difficult to achieve in practice even in calm sea due to the effect of hydrodynamic interaction when the ships are closing in. Furthermore, currents that are present in the lightering zone add to the operational complexity. A field measurement experiment has been carried out with a Velocity Information GPS (VI-GPS) system installed onboard a ferry approaching port for berthing which is similar to an STS lightering. The paper proposes to apply VI-GPS as input sensor to a decision-support and guidance system aiming to provide accurate velocity information to the officer in charge of an STS operation. It is argued that DOP of VI-GPS is related to the velocity error.

1 INTRODUCTION

Applications of ship-to-ship operations for cargo transfer are expected to be increasing. Currently, about 25 percentages of all oil imported to the US comes through lightering operations. An ongoing research program on Ship-To-Ship (STS) operations with focus on STS lightering has a major objective to develop a guidance and decision-support system for the key operative personnel. The initial approach phase can be regarded as a collision avoidance maneuver which aim is to obtain the required safety distance, while the final approach is maneuvering towards the other ship and operation alongside until the ships have been moored together after which cargo transfer can commence. STS operations are individually different because of variations in the environmental conditions and the maneuvering characteristics of ships.

The final approach phase is particularly critical in order to avoid steel to steel contact. The officer in charge of an STS lightering, the Mooring Master, has currently no equipment at his disposal for determining the relative speeds and distances with sufficient accuracies and the decision of adequate maneuvering orders is thus mainly based on visual observations (Pedersen et al. 2008).

The velocity of a movable body can be easily determined by using the GPS receiver generated Doppler measurement or the carrier-phase derived Doppler measurement as long as the satellite velocity is precisely known. The kinematic GPS (K-GPS) is well known to provide accurate positions. Although K-GPS assures high precision measurement in a cm order of magnitude, it is required that the reference station on land is within 20 km of the moveable body (Hou et al. 2005).

A method for precise velocity measurement using Velocity Information GPS (VI-GPS) is described for STS lightering ship. The Doppler measurement generated by GPS receiver is a measure of instantaneous velocity that is measured over a very short time interval, whereas the carrier-phase derived Doppler measurement is a measure of mean velocity between observation epochs. The velocity integration with respect to time is the displacement during a period between the two epochs (Hou et al. 2005).

In this paper, an experiment has been conducted onboard a ship entering port for berthing where the velocity information by VI-GPS was used for measuring precise 3-D velocity (longitudinal, transverse and vertical). The results has been compared with those of K-GPS and evaluated with respect to DOP (Dilution Of Precision) of VI-GPS (Hoffmann-Wellenhof et al. 2004).

2 CONCEPT OF SHIP-TO-SHIP OPERATION

A Ship-To-Ship (STS) transfer operation is an operation where cargo (e.g. crude oil or petroleum products) is transferred between seagoing ships moored alongside each other. Such operations may take place when one ship is at anchor or when both are underway. In general, the operational phases includes the approach maneuver, berthing, mooring, hose connecting, safe procedures for cargo transfer, hose disconnection, unmooring and departure maneuver (ICS & OCIMF, 2005).

In the case of maneuvering alongside with two ships at forward speed, the ship acting as the Ship-To-Be-Lightered maintains steering speed (approximately 5 knots) and keeps a steady course heading. It is normal that the maneuvering ship, also referred to as the Service Ship, approaches and berths with the port side to the starboard side of the STBL.

The other case of maneuvering is that the STBL is at anchor, which is quite common in STS operations. For such operations, the STBL anchors in a pre-determined position using the anchor on the opposite side to where the maneuvering ship will approach. A berthing operation should only be carried out after the ship at anchor is lying on a steady heading with reference to prevailing environmental conditions.

Figure 1 shows the final stage with both ships maneuvering alongside with forward speed in calm seas.

Figure 1. The two ships have come alongside and commenced mooring operation while still underway at slow forward speed. The ships will be brought dead in the water and the STBL is to anchor if the operation takes place in a lightering zone with shallow waters.

3 VELOCITY INFORMATION BY GPS

The observation equation for the GPS carrier phase measurements is the following (Hou, 2005):

$$\Phi = \rho + c \cdot (dt - dT) + \lambda N - d_{ion} + d_{trop} + \varepsilon_\Phi \quad (1)$$

where Φ is the carrier-phase observation; ρ is the geometric distance between a satellite and a receiver; c is the light speed in vacuum; dt, dT are the receiver and satellite clock error; d_{ion}, d_{trop} are the ionospheric and the troposheric delay; ε_Φ is the receiver noise and multipath error.

3.1 Velocity Information GPS (VI-GPS)

The velocity information GPS uses the epoch single difference technique and the first order central difference approximation of the carrier-phase rate.

Time differential observations are obtained by subtracting the observations at the previous epoch, k-1 from those at the present epoch, k. It is assumed that variations of propagation errors in the ionosphere and troposphere are small and negligible when the interval of observations is short. The time differential observation is expressed in the following equation and temporal differences remove the phase ambiguities:

$$\delta\Phi = \delta\rho + c \cdot (\delta dt - \delta dT) + \varepsilon_{\delta\Phi} \quad (2)$$

Here, the symbol δ means the time differential operator, and $\delta\Phi$ is the phase observation in temporal difference between two epochs. In discrete expression of Equation 2, the phase difference between two sequential epochs is measured as following equation:

$$\Phi_k^j \approx \frac{\Phi_{k+\Delta t}^j - \Phi_{k-\Delta t}^j}{2 \cdot \Delta t} \quad (3)$$

where superscript j represents the satellite; k and Δt are the observation epoch and time interval of the observation, respectively. Figure 2 shows the time differential carrier phase measurement by VI-GPS.
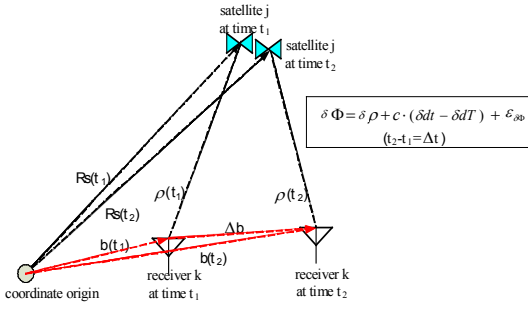

Figure 2. Time differential carrier phase measurement by Velocity Information GPS.

The observation equation can be written as the following:

$$\mathbf{L} = f(\mathbf{X}) + \mathbf{V} \tag{4}$$

$$\mathbf{L} = [\delta\Phi_1, \cdots, \delta\Phi_N]^T$$

$$\mathbf{X} = [\delta\rho_1 + c\cdot(\delta dt_1 - \delta dT), \cdots, \delta\rho_N + c\cdot(\delta dt_N - \delta dT)]^T$$

where $\mathbf{X}$ is the vector of observations; $f(*)$ is the vector of known function mapping $\mathbf{X}$ to $\mathbf{L}$; $\mathbf{X}$ is the vector of unknown parameters; $\mathbf{V}$ is the vector of residuals; subscript N is satellite number; and T is vector transposition.

The equation must be linearized with respect to unknowns before performing the least-squares adjustment. Linearization of Equation 4 is made by replacing the nonlinear functions with their Taylor series approximations at the point an initial value of the solution vector, $\mathbf{X}^0$ and taking only the first order terms.

$$\mathbf{L} - f(\mathbf{X}^0) = \frac{\partial f}{\partial \mathbf{X}} d\mathbf{X} + \mathbf{V} \tag{5}$$

$$\mathbf{W} = \mathbf{A}\mathbf{X} + \mathbf{V} \tag{6}$$

where $\mathbf{W}$ is the misclosure vector, $\mathbf{L} - f(\mathbf{X}^0)$; $\mathbf{A}$ is the design matrix of partial derivatives evaluated using $\mathbf{X}^0$; and the vector of residuals.

Assuming that the matrix $\mathbf{A}$ at the present epoch k is identical to the one at the previous epoch k-l, the least-squares solution of Equation 6 is the displacement between the two epochs. The misclosure vector $\delta\mathbf{W}$ that is obtained from Equation 2 is distinguished from the observation equation for positioning obtained Equation 1.

$$\delta\mathbf{W} = \mathbf{A}\cdot\delta\mathbf{X} + \mathbf{V} \tag{7}$$

When the weight of measurement is not equal, the equation must be weighted with an observation weight matrix $\mathbf{P}$. If the technique with double differ-

ence observation is used, the mathematical correlation has to be taken into account, using the matrix $\mathbf{P}$. The normal matrix $\mathbf{N}$, the vector $\mathbf{U}$ and the least-squares solution are derived from the application of the least-squares principle ($\hat{\mathbf{V}}^T \mathbf{P} \hat{\mathbf{V}} \to$ min.) to Equation 7 as follows:

$$\mathbf{N} = \mathbf{A}^T \mathbf{P} \mathbf{A} \tag{8}$$

$$\mathbf{U} = \mathbf{A}^T \mathbf{P} \delta\mathbf{W} \tag{9}$$

$$\delta\hat{X} = \mathbf{N}^{-1}\mathbf{U} \tag{10}$$

Observation at a one second interval gives a solution for unit displacement, i.e. velocity. Using the position from absolute positioning with a single GPS receiver as a prior position, the least-squares solution provides the correction to the a priori position.

3.2 Kinematic GPS (K-GPS)

The kinematic GPS uses the double differences technique and the carrier phase observation equation is the following (Tatsumi, 2008):

$$\Delta\nabla\Phi = \Delta\nabla\rho + \Delta\nabla d\rho + \Delta\nabla\lambda N - \Delta\nabla d_{ion} + \Delta\nabla d_{trop} + \varepsilon_{\Delta\nabla\Phi} \tag{11}$$

where $\Delta\nabla$ is the double difference operator. The double differences technique needs two receivers. The reference station is set as a fixed point on land, while the rover station is set on the movable body. When the distance between the two stations are within 20 km, the orbital and atmospheric errors, $\Delta\nabla d\rho$, $\Delta\nabla d_{ion}$ and $\Delta\nabla d_{trop}$ are illuminated. Equation 11 then becomes as follows:

$$\Delta\nabla\Phi = \Delta\nabla\rho + \Delta\nabla\lambda N + \varepsilon_{\Delta\nabla\Phi} \tag{12}$$

It is well known that over four double differences carrier phase observations from four satellites can decide precise kinematic GPS 3-D position of the rover station, $\mathbf{P}_{rover}$. The velocity of the movable body is calculated from the time differential operation of this precise rover 3-D position as follows:

$$\mathbf{V} \approx \Delta\mathbf{P} = \frac{\mathbf{P}_{rover}^{k+\Delta t} - \mathbf{P}_{rover}^{k-\Delta t}}{2\cdot\Delta t} \tag{13}$$

4 SIMULATED STS OPERATION

A simulated STS operation was carried out with a ferry on 17th of September, 2007 when it was entering the Sibusi port of Kagoshima prefecture that is located in southwest of Japan. Figure 3 shows the experimental area overview. The ferry was equipped with two GPS receivers that were located on stern and bow, respectively.
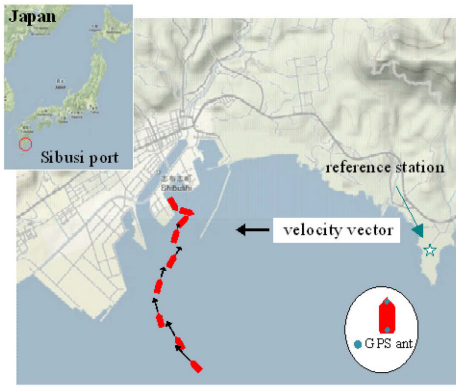
Figure 3. Experimental area overview of Sibusi port.

Table 1. General specification of the ferry, data details and experimental conditions.

Gross tonnage	12,418 [tons]
Service speed	23.0 [knots]
Length overall	186.0 [m]
Width	25.5 [m]
Sampling frequency	5 [Hz]
No. of data samples	8000
No. of GPS satellites	7
(satellites no.)	(no. 5, 9, 12, 14, 18, 22, 30)

The first part (800 sec) of the approach was similar to a STS maneuver with the STBL at anchor. It should be noted that during the time range around 800-1300 seconds the ferry turned backward to the berth, which is a maneuvering that is not taking place in any STS operation. The reference station was about 3 km apart from the berth while the maximum distance from the ferry (rover station) was 7 km. (It is well known that K-GPS accuracy has cm order if the reference station is within 20 km from the rover station.)
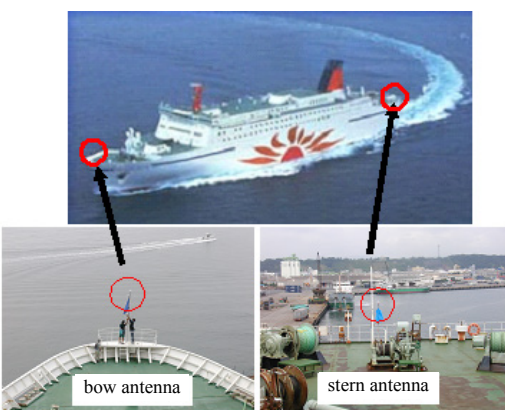

Figure 4. The ferry and positions of GPS receivers.

Table 1 shows the general specification of the ferry, data details and experimental conditions. The experimental period was about 27 minutes from standby for entering port until stop engine order with 5 Hz data sampling frequency. The number of data samples was 8000 recorded by PDA (Personal Digital Assistance), and each GPS receiver processed the same GPS signals transmitted by 7 GPS satellites.

Figure 4 shows the ferry and the two GPS receivers set on the bow and stern side.

K-GPS data was calculated from the reference station data to rover station while VI-GPS data was calculated from rover station alone. In this paper, the velocity by K-GPS is defined as a standard velocity, and then the velocity error subtracts K-GPS velocity results from VI-GPS results.

4.1 Experimental results

Figures 5-7 show the results of longitudinal, transverse and vertical velocity components of bow, respectively.
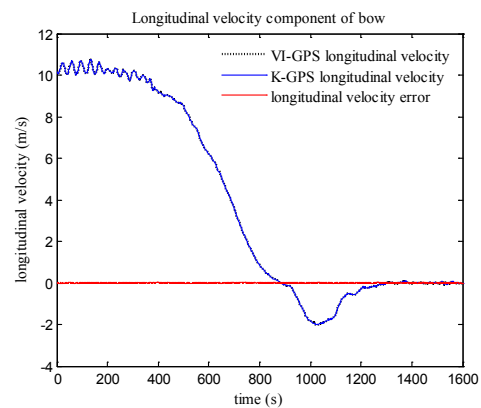

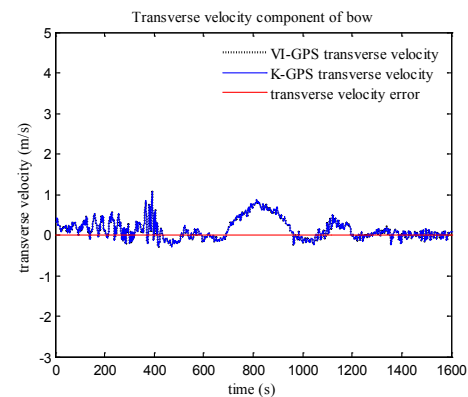
Figure 5. Longitudinal velocity component of bow.

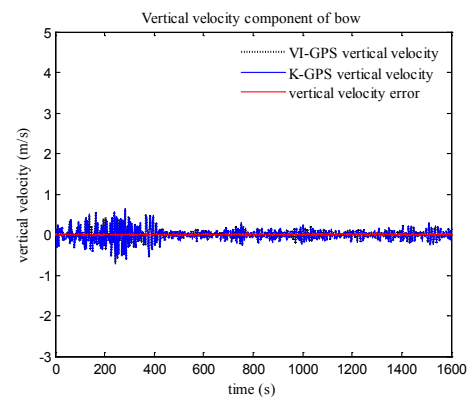Figure 6. Transverse velocity component of bow.

Figure 7. Vertical velocity component of bow.

Figure 5 shows the longitudinal velocity components by VI-GPS with black dot line, K-GPS with

blue line and longitudinal velocity error with red line subtracted the longitudinal velocity component by K-GPS from VI-GPS result. The velocity is decreasing from around 11 m/s to zero during the recorded logging time. The velocity is oscillating the first 400 seconds which is due to low frequency waves (swell) outside the breakwater. As is shown, the two results by VI-GPS and K-GPS show a good correspondence. Figure 6 shows the transverse velocity components of bow. VI-GPS and K-GPS results also show a good correspondence, and similar to the longitudinal velocity results. Figure 7 shows the vertical velocity component and the velocity error also has a small difference.
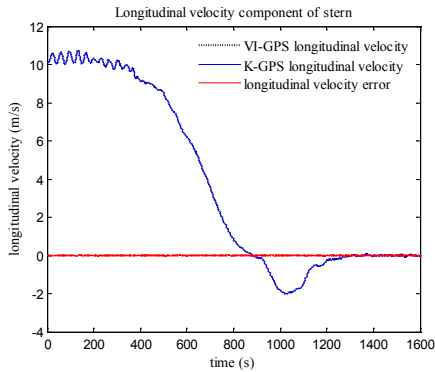

Figure 8. Longitudinal velocity component of stern.
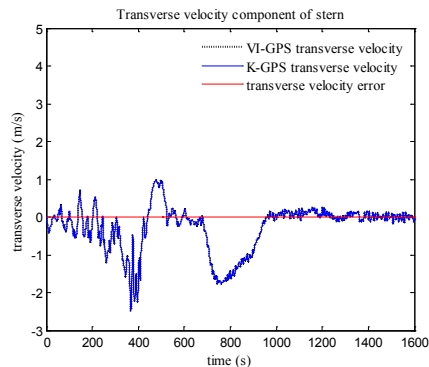

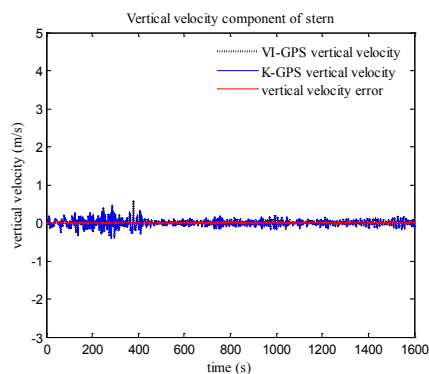Figure 9. Transverse velocity component of stern.

Figure 10. Vertical velocity component of stern.

Figures 8-10 show the results of longitudinal, transverse and vertical velocity components of stern, respectively. Figure 8 shows the longitudinal velocity components by VI-GPS with black dot line, K-GPS with blue line and velocity error with red line

subtracted K-GPS results from VI-GPS results. The results are oscillating during the first 400 seconds due to the swell. Two results by VI-GPS and K-GPS show a good correspondence, similar to the bow results, and its velocity error also shows smaller difference compared to the longitudinal velocity error. Figure 9 shows the transverse velocity component of stern. As same with the results of bow, it shows a good correspondence with VI-GPS and K-GPS results. Figure 10 shows the result of vertical velocity component of stern. The results show a good correspondence between VI-GPS and K-GPS results, and the vertical velocity error subtracted K-GPS results from VI-GPS results shows small difference.

Table 2 is the results of longitudinal, transverse and vertical velocity errors subtracted K-GPS results from VI-GPS results. From the results, the velocity errors of bow side show slightly higher standard deviation values than stern side velocity errors. Among the velocity errors at bow, the vertical velocity error shows the largest standard deviation value with 0.72 cm/s. The vertical velocity error at stern also shows large value with 0.70 cm/s standard deviation.

Table 2. Longitudinal, transverse and vertical velocity errors of bow and stern sides.

Bow	Longitudinal V-error	Transverse V-error	Vertical V-error
Mean (cm/s)	-0.03	-0.13	-0.06
Std (cm/s)	0.24	0.22	0.72
Stern			
Mean (cm/s)	-0.04	-0.13	-0.07
Std (cm/s)	0.22	0.21	0.70

4.2 Considerations

From the results showing bow velocity errors the standard deviations of longitudinal, transverse and vertical velocity errors have been analyzed. In order to identify the relation between velocity errors and DOP (Dilution Of Precision), DOP changes of VI-GPS was also examined as well as the relation with bow velocity errors.
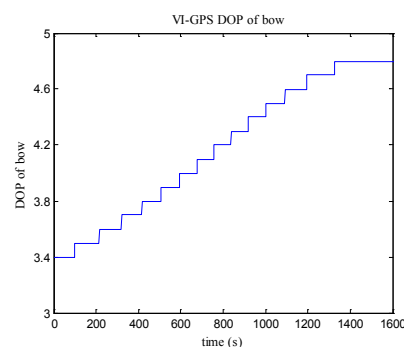

Figure 11. VI-GPS DOP of stern side.

Figure 11 shows how the VI-GPS DOP changes at the bow side. DOP is increasing according to time

progression from 3.4 to 4.8. Figure 12 shows the relation between bow velocity errors and DOP changes of VI-GPS divided into every 100 seconds. In the figure, blue Δ, red • and black + symbols show the standard deviation of longitudinal, transverse and vertical velocity errors with respect to DOP changes, respectively. According to the increase of DOP, the standard deviation of longitudinal and vertical velocity errors are increasing, but the transverse velocity error does not show a particular increase according to DOP changes compared to other velocity errors. As shown in Figure 12, VI-GPS can be used with a good accuracy within 1 cm/s standard deviation if DOP could be obtained under 4.8.
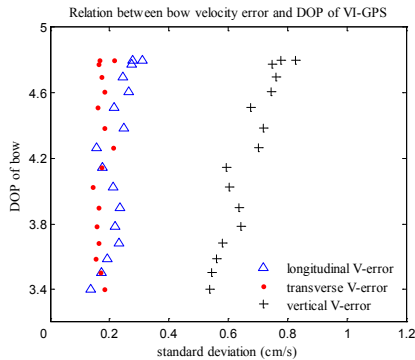

Fig 12. Relation between bow velocity error and DOP of VI-GPS.

Table 3. Standard deviation of longitudinal, transverse and vertical velocity errors with respect to DOP changes of bow.

Data no. (sec)	DOP	Longitudinal std (cm/s)	Transverse std (cm/s)	Vertical std (cm/s)
1-200	3.4-3.5	0.14	0.18	0.54
101-200	3.5	0.17	0.17	0.54
201-300	3.5-3.6	0.19	0.15	0.56
301-400	3.6-3.7	0.23	0.16	0.58
401-500	3.7-3.8	0.22	0.16	0.64
501-600	3.8-4.0	0.24	0.16	0.63
601-700	4.0-4.1	0.21	0.14	0.60
701-800	4.1-4.2	0.17	0.17	0.59
801-900	4.2-4.3	0.16	0.21	0.70
901-1000	4.3-4.4	0.25	0.18	0.72
1001-1100	4.4-4.6	0.22	0.16	0.68
1101-1200	4.6-4.7	0.27	0.18	0.74
1201-1300	4.7	0.24	0.17	0.76
1301-1400	4.7-4.8	0.27	0.16	0.75
1401-1500	4.8	0.28	0.22	0.78
1501-1600	4.8	0.31	0.17	0.83

In the final approaches of STS lightering operation, the longitudinal and transverse velocity information is very important for the mooring master. Therefore, more precise relation between DOP and longitudinal, transverse velocity errors has been shown in Table 3 with vertical velocity error as well. Table 3 shows the standard deviations of longitudinal, transverse and vertical velocity errors with respect to DOP changes of VI-GPS at bow. The velocity error shows a small standard deviation within 1 cm/s when DOP is under 4.8. The vertical velocity error has increased gradually according to DOP increase from 0.54 to 0.83 cm/s. Even though, it shows

high values of 0.83 cm/s with maximum velocity error compared to other velocity errors, it is considered that VI-GPS has an enough accuracy under 1 cm/s. Furthermore, because the longitudinal and transverse velocities are mainly used as important information in the final approaches of STS lightering operation, the vertical velocity error can be negligible.

5 CONCLUSIONS

STS operations represent a challenge to the officer in charge because currently there is no equipment implemented that can provide the relative speeds and distances with sufficient accuracies. Decision of adequate maneuvering orders is then based on visual observations. VI-GPS has been applied to measure precise 3-D velocity (longitudinal, transverse and vertical) for STS operations. The advantage is that precise accuracy is not limited to distances within 20 km as the case of K-GPS.

An experiment representing a simulated STS operation was done in Sibusi port of western Japan during entering the port. The results of VI-GPS velocity showed a good correspondence with K-GPS velocity results, i.e. within 1 cm/s.

From the result of relation between bow velocity errors and DOP of VI-GPS, 3-D velocity by VI-GPS has precise accuracy within 1 cm/s level compared to K-GPS if DOP of VI-GPS can be obtained under 4.8. The longitudinal and transverse velocity of bow side showed standard deviation of 0.24 and 0.22 cm/s, respectively. It is considered that VI-GPS has sufficient accuracy to serve as sensor input for providing relative velocities in a decision-making and guidance system tailored for STS operations.

REFERENCES

Hoffmann-Wellenhof, B., Lichtenegger, H. and Collins, J. 2004. *Global Positioning System: Theory and Practice*, New York: Springer-Verlag Wein.
Hou, D., Yoo, Y., Kouguchi, N., Ishida, H., Fujii, H. and Itani, K. 2005. Experimental Results of Comparison between Velocity Integration and OTF Position on the Sea, *Institute of Navigation National Technical Meeting (ION NTM 2005), San Diego, 24-26 January 2005*.
ICS & OCIMF, 2005. *Ship to Ship Transfer Guide (Petroleum)*, International Chamber of Shipping & Oil Companies International Marine Forum, London: Witherbys.
Pedersen, E., Shimizu, E. and Berg, T.E. 2008. Navigational Challenges for Ships Operating in Close Proximity, International Conference on Safety and Operations in Canals and Waterways (SOCW 2008), Glasgow, 15-16 September 2008.
Tatsumi, K., Kouguchi, N., Yoo, Y., Kubota, T. and Arai, Y. 2008. Precise 3-D Vessel Velocity Measurement for Docking and Anchoring, *International Offshore and Polar Engineering Conference (ISOPE 2008), Vancouver, 6-11 July 2008*